EPJ Web of Conferences **40**, 15002 (2013)
DOI: 10.1051/epjconf/20134015002

Metamagnetic transition in Tb_2MnCoO_6.

V. Cuartero[1], J. Blasco[2], J. García[2], J. A. Rodríguez-Velamazán[2,3], and C. Ritter[3]

[1]ALBA Synchrotron/CELLS, 08290 Cerdanyola del Vallès, Spain
[2]Instituto de Ciencia de Materiales de Aragón, Departamento de Física de la Materia Condensada, CSIC-Universidad de Zaragoza, 50009 Zaragoza, Spain
[3]Institute Laue-Langevin, Boîte Postale 156, 38042 Grenoble Cedex 9, France

Abstract. The magnetic properties of the double perovskite Tb_2MnCoO_6 have been studied. The refinement of neutron pattern reveals *antisite* defects in the ordered array of Mn^{4+} and Co^{2+} cations. The temperature dependence of dc magnetization exhibits a magnetic transition at ~100 K with a strong irreversibility between ZFC and FC conditions. The ac magnetic susceptibility curve shows a strong peak at the same temperature whose position and intensity slightly depends on the field frequency. These features are typical of a spin-glass-like phase but neutron diffraction shows the onset of a ferromagnetic contribution at the same temperature. Ferromagnetism in this sample is associated to superexchange interaction between Mn^{4+} and Co^{2+} cations. The most striking property of Tb_2MnCoO_6 is the presence of field induced transitions. This is observed in the magnetic hysteresis loops below 100K. The metamagnetic transition was studied by powder neutron diffraction at different temperatures and magnetic fields. At low temperature, the magnetic field induces a long range magnetic ordering of Tb^{3+} moments in the *ab*-plane. The magnetic peaks of Tb moments at 30 kOe vanish at 60 K. Above this temperature, the metamagnetic transition is ascribed to the field induced transition from short to long range ferromagnetic ordering in the Mn-Co sublattice.

1 Introduction

Multiferroic oxides with magnetoelectric coupling are promising candidates in the field of information technology [1], but they are rare because conventional mechanisms of ferroelectricity in oxides do not allow strong magnetic interactions [2]. Consequently, unusual types of induced ferroelectricity are now being explored [2]. One of these new approaches is the predicted ferroelectricity induced by E-type antiferromagnetic ordering [3] which was first reported in orthorhombic $HoMnO_3$ [4]. Recently, a related magnetic structure has been found in the Lu_2MnCoO_6 double perovskite showing multiferroic behaviour at low temperature [5]. This result encourages the study of other double perovskites with heavy rare-earth.

We here report a thorough study on the magnetic properties of Tb_2MnCoO_6 compound which also adopts the structure of a double perovskite. A previous study on $TbMn_{0.5}Co_{0.5}O_{3.06}$ reported metamagnetic behaviour ascribed to a transformation from a spin-glass to ferromagnetic (FM) phase induced by the magnetic field [6]. Metamagnetism is related to the strong magnetoelectric effect of the parent compound, $TbMnO_3$. This is multiferroic due to the non-collinear cycloidal magnetic ordering of Mn moments which induces ferroelectricity [7]. Tb^{3+} moments are ordered at low temperature coupled to the Mn sublattice. The application of a magnetic field induces a metamagnetic transition in the ordering of Tb moments modifying both the cycloid and the polarization directions [7,8]. This effect reveals the importance of Mn-Tb coupling in the multiferroic properties. Perturbation of the Mn sublattice by partial replacing with non-magnetic cations [9,10] or Co [11] is very detrimental for the Mn-Tb coupling and hence, for multiferroic properties. In $TbMn_{1-x}Co_xO_3$ compounds, small replacements have a dramatic effect as this substitution is not isovalent because the formal equilibrium Mn^{3+}-Co^{3+}⇋ Mn^{4+}-Co^{2+} is not completely shifted to the right in these perovskites [11]. The presence of mixed valence cations favours competitive magnetic interaction in $TbMn_{1-x}Co_xO_3$.

2 Experimental section

The sample was synthesized by ceramic method. Tb_4O_7, $MnCO_3$ and Co_3O_4 were mixed and heated at 1000 ºC for 12 h in air. The resulting powder was pressed into a pellet and heated at 1100º C/24 h, 1200ºC/48 h and 1300º C/24 h with intermediate grindings and repressing. In the last step, the sample was cooled at 24ºC/h down to room temperature. The oxygen content was tested by cerimetric

titration showing the nominal oxygen content within the experimental error (±0.01). X-ray diffraction pattern was collected at room temperature using a Rigaku D/max-B diffractometer and Cu K_α wavelength. The x-ray pattern agrees with a perovskite single phase.

Neutron diffraction experiments have been performed using the high intensity D1B (λ=2.52 Å) instrument at the ILL (Grenoble, France). The patterns were measured at zero field between 2 and 200 K. A cryomagnet was coupled to the experimental setup in order to acquire patterns at selected temperatures up to 30 kOe. FULLPROF was used to analyze all patterns [12].

A commercial squid magnetometer (MPMS, Quantum Design) was used to determine the macroscopic magnetic properties of the sample between 5 and 300 K. DC magnetization in zero-field-cooled (ZFC) and field-cooled conditions were determined at 500 Oe. AC magnetic susceptibility was also measured at several frequencies with an alternating field of 4 Oe.

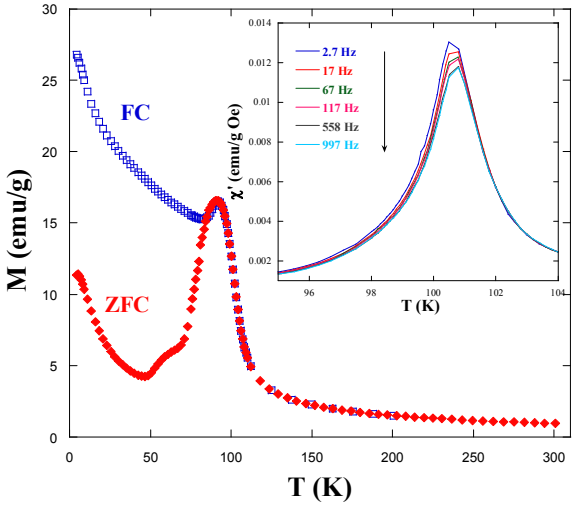

Fig. 1. Temperature dependence of magnetization for Tb_2MnCoO_6 under FC and ZFC conditions at 500 Oe. Inset: In-phase ac magnetic susceptibility of this sample at selected frequencies.

3 Results and conclusions

Figure 1 shows the temperature dependence of magnetization for Tb_2MnCoO_6 under ZFC and FC conditions at 500 Oe. The ZFC curve exhibits a broad peak at 90 K and an increase of magnetization below 50 K which can be ascribed to the paramagnetic contribution of Tb^{3+} cations. The FC branch increases as temperature decreases with a small kink around the ZFC peak where both branches meet. The sudden increase of FC curve at ~100 K resembles a FM transition but the strong magnetic irreversibility exhibited by this sample is a signature of magnetic inhomogeneity. The inset of figure 1 shows the real component of ac magnetic susceptibility around the magnetic transition at different frequencies of the alternating field. A clear peak, showing magnetic relaxation, can be observed. The peak is shifted to higher temperatures and its amplitude decreases as the frequency increases. This property agrees with the existence of glassy magnetic behaviour [13].

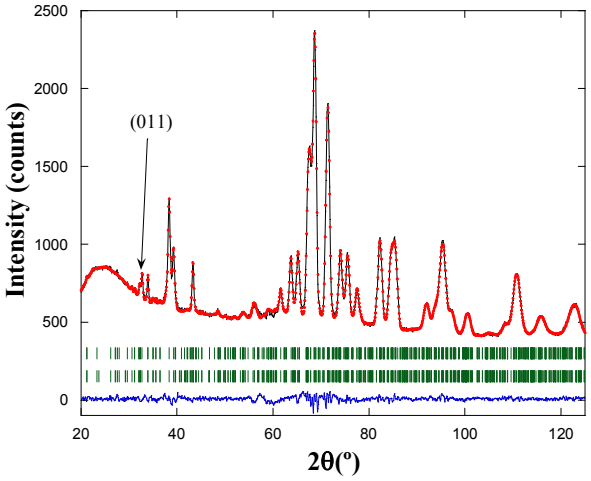

Fig. 2. Rietveld refinement of the neutron pattern of Tb_2MnCoO_6 at 2 K (**H**=0). The first reflection typical of $P2_1/n$ space group is marked with an arrow.

In order to gain insight into the magnetic ground state of this sample, neutron diffraction patterns were collected between 200 and 2 K. All the neutron patterns reveal the existence of (011) reflection (see figure 2) which is forbidden in the *Pbnm* space group. This result reveals that Tb_2MnCoO_6 belongs to the family of double perovskites with an ordered sequence of Mn and Co atoms in the perovskite B-sublattice. Rietveld refinement indicated that this ordering is not perfect [11] but the existence of 25.5±1% of *anti-site* defects (AS) is observed. AS refers to miss-placed atoms (Co atoms at Mn position and *vice versa*, 50% means simple perovskite).

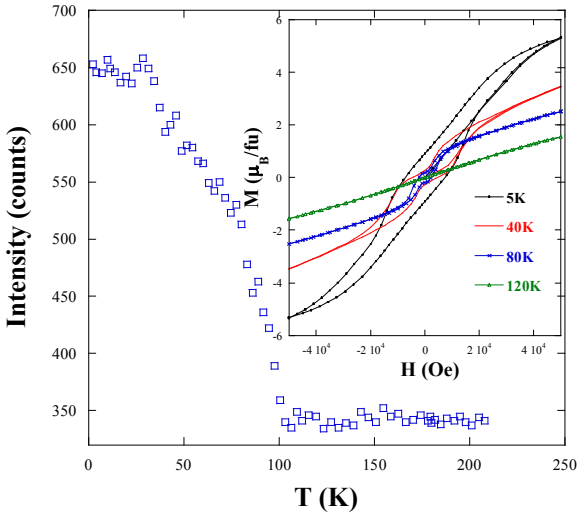

Fig. 3. Temperature dependence of the first FM peaks, (110)+(002), for Tb_2MnCoO_6 at zero field. Inset: Magnetic hysteresis loops for the $TbMn_{1/2}Co_{1/2}O_3$ formula unit.

Below 100 K, the intensity of some reflections grows as shown in figure 3. It agrees with the developing of a FM long range ordering. The presence of spontaneous magnetization is confirmed by the presence of hysteresis loops in the isothermal magnetization below 100 K (see inset of figure 3). The hysteresis loops show a strong

coercive field at 5 K. The magnetization does not achieve saturation at 50 kOe and the value of the magnetic moment at this field is higher than the one expected from a full polarized Mn-Co sublattice as we will see later on. This suggests that Tb polarization also plays an important role in the magnetic properties of this sample. Coercivity decreases with increasing the temperature but the most striking point is the presence of metamagnetic transitions with the associated plateaus clearly noticeable in the measurements at 40 and 80 K.

Figure 4 shows the patterns obtained at 2 K and at three different magnetic fields. At zero field, the Rietveld refinement (see figure 2) suggests a similar magnetic moment for Mn and Co so only one value was refined improving the convergence of the fit. The refinement yielded values of $\boldsymbol{\mu}_{Mn}=\boldsymbol{\mu}_{Co}$ = 2.17(4) μ_B with the moment located in the *xz*-plane. This situation with the same magnetic moment for both 3d metals agrees with a high spin configuration for Mn^{4+} and a low spin one for Co^{2+}. In both cases **S**=3. The refinement improves (R_M=4.9%) considering a minor component for Tb^{+3} moments, $\boldsymbol{\mu}_{Tb}$ = 0.22(4) μ_B, which is antiferromagnetically coupled to the Mn and Co moments in agreement with the negative *d-f* coupling [6]. The main contribution of Tb^{3+} moments seems to be of short range as shown by the broad bump at low 2θ values that resemble the short ordering of Tb^{3+} moments in related compounds [11].

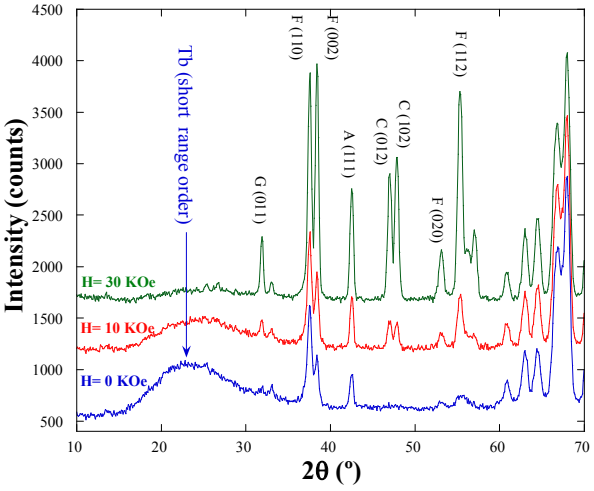

Fig. 4. Neutron patterns for Tb_2MnCoO_6 at 2 K and at the indicated magnetic fields. The patterns have been shifted upwards for the sake of comparison. Some magnetic reflections are labelled following the Bertaut's notation [14].

An external magnetic field induces the growth of some peaks as observed in figure 4. These peaks agree with a propagation vector **k**=(0,0,0) and, following the Bertaut's notation [14], they correspond to the four common magnetic reflections in perovskite compounds, labelled as A-, F-, C- and G-types. Nevertheless, the most significant increase corresponds to the F- and C-type reflections. The diffuse scattering associated with the short ordering of Tb^{3+} vanishes simultaneously with the appearance of the new reflections suggesting a reordering of these moments. This behaviour of Tb_2MnCoO_6 resembles the properties of other Tb-based compounds. Due to a strong Ising anisotropy, Tb^{3+} usually orders in non collinear arrangements in the *ab*-plane[15] and a magnetic field induces realignment of the moments. The strong anisotropy of Tb^{3+} moments implies that the magnetic configuration of this cation in a particular grain strongly depends on the grain orientation respect to the external magnetic field, in turn correlated with the geometry of the diffraction process. Therefore, a quantitative analysis from powder diffraction under a magnetic field is a very hard task. However, a qualitative approach would be useful to gain insights into the nature of this metamagnetic transition.

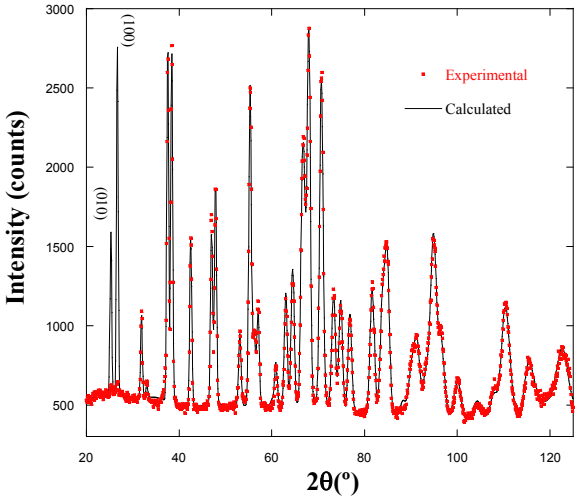

Fig. 5. Neutron pattern of Tb_2MnCoO_6 at 2 K and 30 kOe together to the simulation performed using $F_{x,y}C_{y,x}$ configurations (see text).

Recently, we have studied metamagnetic transitions in a $TbMn_{0.9}Al_{0.1}O_3$ single crystal for **H**||**b** [16]. The high field phase adopted by Tb^{3+} moments can be described as C_xF_y in the Bertaut's notation [14]. Presumably, the ordering adopted for **H**||**a** would be F_xC_y as observed in related compounds [17]. In the present sample, both configurations can also be present and, in addition, polarization of Tb moments along the *z*-direction for **H**||**c** cannot be discarded. With these premises, we have simulated the neutron patterns for an even mixture of Tb^{3+} moments adopting C_xF_y and F_xC_y magnetic orderings. The results were promising as we could reproduce the increase of the observed magnetic reflections including the A- and G- types. Then, we have included a third phase with a FM component along the *z*-direction. Regarding the Mn and Co moments, they are FM ordered showing an antiferromagnetic coupling to FM component of Tb^{3+} moments in the *xy*-plane. Along the *z*-direction, the best simulation is obtained with a positive coupling. The comparison between experimental and best simulated pattern is plotted in figure 5.

Two things attract much attention in the simulation of figure 5. First of all, the nearly perfect fit for most of the pattern and secondly, the strong discrepancy for the two first magnetic peaks which correspond to the first C-type magnetic reflections, (010) and (100). The latter can be understood in basis to the geometry of the diffraction process as indicated in figure 6. In this picture, we represent the diffraction condition for the (010) reflection. When this condition is fulfilled, **H** is

perpendicular to the scattering vector **Q**. The (010) magnetic reflection becomes allowed for a C_xF_y configuration of the Tb^{3+} moments which is formed when **H**||**b** (or **H**||**Q** in figure 6) but this geometry cannot be fulfilled in our experimental setup. For **H**⊥**b** Tb^{3+} adopts other configurations (F_xC_y or F_z) and the intensity of (010) reflection becomes null. Similar geometric extinction can be inferred for the (100) reflection and the F_xC_y configuration. In spite of this limitation, the rest of the neutron pattern nicely agrees with the proposed mixture of configurations which is already observed in related Tb-perovskites [16,17] so we can hypothesize that metamagnetic transitions al low temperature comes from the field induced transition of the Tb^{3+} moments within the *xy*-plane following two main directions [15].

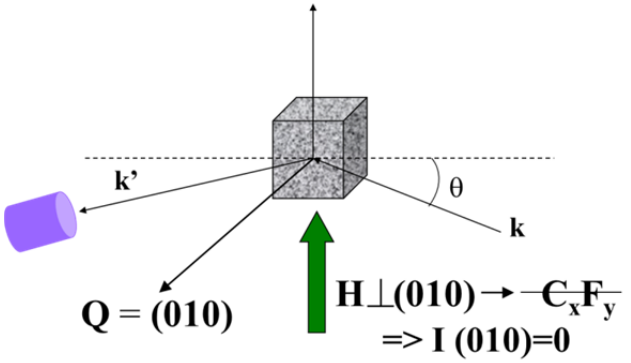

Fig. 6. Geometry for diffraction measurement at D1B under an external magnetic field. **H** is perpendicular to the plane composed by scattering vector **Q** and neutron beam (indicated by the vectors **k**). The picture shows the arrangement for the scattering of (0 1 0) planes which is detrimental for the C_xF_y order and the intensity of (0 1 0) reflection becomes null.

The temperature dependence of the magnetic reflections at 30 kOe was monitored at selected temperatures. The evolution of representative reflections is plotted in the figure 7. Clearly, A-, G- and C-type reflections vanish at 60 K. Above this temperature, only F-type reflections have a significant contribution to the neutron pattern although a strong intensity decrease is also observed on warming from 2 up to 40 K. These results indicate that long range magnetic ordering of Tb^{3+} vanishes at ~60 K for H=30 kOe. Above this temperature, FM comes from Mn-Co sublattice. However, metamagnetic transitions are still present in this sample above 60 K (see hysteresis loop at 80 K in fig. 3) so another mechanism independently of Tb^{3+} reordering must operate in this compound. The refinements of the neutron patterns following the abovementioned FM ordering of Mn-Co atoms yielded a refined magnetic moment of 1.38(9), 2.10(5) and 2.56(5) μ_B per transition metal for H=0, 10 and 30 kOe, respectively. Therefore, the increase of H favours the long range FM region, probably at the expense of a decrease of glassy regions with short range FM interactions. The different types of metamagnetic transitions might be related to the different shape (coercivity) of the hysteresis loops (Fig. 3).

In conclusion, Tb_2MnCoO_6 is a double perovskite with a significant number of AS defects. The structural disorder leads to competitive interactions giving rise to magnetic inhomogeneity. Coexistence of long- and short-range FM ordering of Mn and Co moments is inferred in this compound from macroscopic measurements. It presents metamagnetic transitions in a wide temperature range showing different kind of magnetic hysteresis loops. Above 60 K, the growth of FM clusters induced by the field seems to account for experimental results. Below 60 K, the magnetic field induces a long range ordering of Tb^{3+} following $F_{x,y}C_{y,x}$ configurations.

The authors thank ILL and Spanish CRG D1B for granting beam time. This work was supported by MICINN (project, FIS08-03951, MAT2007-61621) and DGA (CAMRADS).

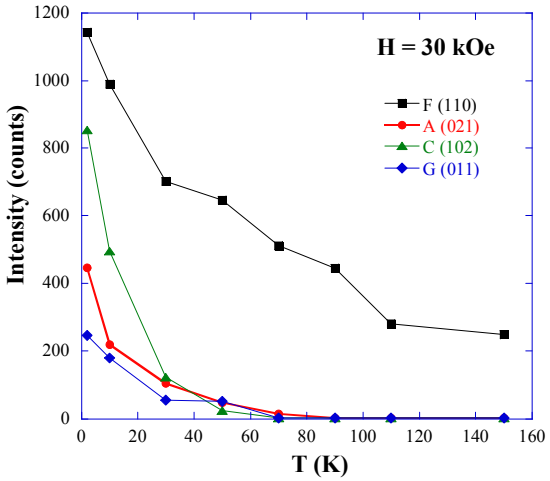

Fig. 7. Temperature dependence of selected magnetic reflections under an external magnetic field of 30 kOe. The type of reflections is indicated in the plot.

References

1. K. F. Wang, J.-M. Liu, Z. F. Ren, Adv. Phys. **58**, 321 (2009).
2. N. A. Hill, J. Phys. Chem. B **104**, 6694 (2000).
3. I. A. Sergienko, C. Sen, E. Dagotto, Phys. Rev. Lett. **97**, 227204 (2006).
4. A Muñoz *et al.* Inorg. Chem. **40**, 1020 (2001).
5. S. Yañez-Vilar *et al.* Phys. Rev. B **84**, 134427 (2011).
6. V. A. Khomchenko *et al.* J. Phys.:Condens. Matter **18**, 9541 (2006).
7. T. Kimura *et al.* Nature (London) **426**, 55 (2003).
8. N. Aliouane *et al.* Phys. Rev. Lett. **102**, 207205 (2009).
9. O. Prokhnenko, *et al.* Phys. Rev. B **81**, 024419 (2010).
10. V. Cuartero *et al.* Phys. Rev. B **81**, 224117 (2010).
11. V. Cuartero *et al.* J. Phys.:Condens. Matter, **24**, 455601 (2012).
12. J. Rodríguez-Carvajal, Physica B **192**, 55 (1993).
13. K. De *et al.* J. Phys.D:Appl. Phys. **40**, 7614 (2007).
14. E. F. Bertaut, J. de Physique Colloque **C1**, 462 (1971).
15. J. Mareschal *et al.* J. Appl. Phys. **39**, 1364 (1968).
16. V.Cuartero *et al.* Phys. Rev. B **86**, 104413(2012).
17. L. Holmes *et al.* J. Appl. Phys **39**, 1373 (1968).